Published online 23 July 2011 *Nucleic Acids Research, 2011, Vol. 39, No. 20* ***8803–8819***
doi:10.1093/nar/gkr557

Tup1 stabilizes promoter nucleosome positioning and occupancy at transcriptionally plastic genes

Jason M. Rizzo[1], Piotr A. Mieczkowski[2] and Michael J. Buck[1,3,*]

[1]Department of Biochemistry and Center of Excellence in Bioinformatics and Life Sciences, State University of New York at Buffalo, NY 14203, [2]Department of Genetics, Carolina Center for the Genome Sciences and Lineberger, Comprehensive Cancer Center, University of North Carolina, Chapel Hill, NC 27599 and [3]Molecular Epidemiology and Functional Genomics, Roswell Park Cancer Institute, Buffalo, NY, 14263, USA

Received December 15, 2010; Revised June 13, 2011; Accepted June 17, 2011

ABSTRACT

Despite technical advances, the future of chromatin mapping studies requires an ability to draw accurate comparisons between different chromatin states to enhance our understanding of genome biology. In this study, we used matched chromatin preparations to enable specific and accurate comparisons of *Saccharomyces cerevisiae* chromatin structures in the presence and absence of the co-repressor protein Tup1. Analysis of wild-type and *tup1 Δ* chromatin data sets revealed unique organizational themes relating to the function of Tup1. Regulatory regions bound by Tup1 assumed a distinct chromatin architecture composed of a wide nucleosome-depleted region, low occupancy/poorly positioned promoter nucleosomes, a larger number and wider distribution of transcription factor-binding sites and downstream genes with enhanced transcription plasticity. Regions of Tup1-dependent chromatin structure were defined for the first time across the entire yeast genome and are shown to strongly overlap with activity of the chromatin remodeler Isw2. Additionally, Tup1-dependent chromatin structures are shown to relate to distinct biological processes and transcriptional states of regulated genes, including Tup1 stabilization of Minus 1 and Minus 2 promoter nucleosomes at actively repressed genes. Together these results help to enhance our mechanistic understanding of Tup1 regulation of chromatin structure and gene expression.

INTRODUCTION

The organization of eukaryotic DNA into chromatin is known to have far-reaching implications on the accessibility and functionality of genetic information stored in the nucleotide sequence (1–3). Eukaryotic genomes are packaged through the wrapping of 147-bp segments of DNA around histone proteins arranged in octamers known as nucleosomes (4,5). Multiple isoforms of the histone proteins can combine to form a number of distinct nucleosome octamers (6–8). Additionally, histones can undergo an assortment of covalent modifications to further diversify the chromatin landscape (9).

The coiling of each 147-bp DNA segment around a nucleosome spans approximately 1.7 helical turns and establishes important topological relationships between the nucleotide sequence and its local chromatin environment (5,10). Nucleosome positioning relative to underlying DNA sequences controls the access of regulatory factors to their genomic-binding locations and helps to coordinate expression programs *in vivo* (11–13). Consequently, the strength of each nucleosome's interaction with its associated DNA sequence can influence gene expression (14,15).

In yeast and other eukaryotes, nucleosome positioning is controlled by a combination of inputs. Rigid poly(A) tracts of DNA serve as nucleosome-excluding sequences and help direct the formation of nucleosome-depleted regions (NDRs) both *in vivo* and *in vitro* (15–19). Chromatin architecture is also believed to be influenced by statistical packing principles whereby well-positioned nucleosomes help organize the regular positioning of nucleosomes in adjacent large stretches of DNA (20–22). In addition to sequence-based considerations and packing rules, a number of protein complexes can actively position nucleosomes to regulate chromatin structure and transcription (2,23–25). The Tup1–Ssn6 corepressor in *Saccharomyces cerevisiae* is one such complex, soliciting several chromatin-mediated mechanisms to regulate gene expression *in vivo* (26).

In yeast, Tup1–Ssn6 is a global repressor of transcription, responsible for the repression of more than 180 genes involved in diverse signaling pathways (27,28). Tup1–Ssn6 was one of the first corepressor complexes to be identified (29), and has since served as a model for similarly

*To whom correspondence should be addressed. Tel: +1 716 881 7569; Fax: +716 849 6655; Email: mjbuck@buffalo.edu

structured corepressor proteins in other eukaryotes, including the *Drosophila* Groucho (Gro) protein, and the mammalian transducin β-like/transducin β-like related (TBL/TBLR) proteins and transducin-like enhancer of split (TLE) proteins (26,27,30). The Tup1–Ssn6 corepressor complex does not bind directly to DNA, but instead is recruited to promoters by sequence-specific DNA-binding proteins which coordinate the expression of specific subsets of genes (27). Upon recruitment to promoters, Tup1–Ssn6 is known to repress downstream genes through several mechanisms, including interfering with the recruitment of transcription machinery, histone deacetylase (HDAC) recruitment, and the establishment of nucleosome positioning (26). Chromatin-dependent mechanisms of Tup1 repression (nucleosome positioning and HDAC recruitment) are not mutually exclusive and redundant repression mechanisms are observed at many Tup1-regulated promoters (31). Moreover, unequal sensitivities of Tup1-regulated genes to the inactivation of different repression pathways *in vivo* suggests that responses to Tup1 repression may vary in a gene-specific fashion, whereby different groups of genes have evolved different strategies for utilizing Tup1–Ssn6 repression mechanisms. Genes that have developed a strong reliance on Tup1-dependent nucleosome positioning for repression *in vivo* have been well characterized by site-specific studies. Of the more than 100 genes regulated by Tup1 only a few have been characterized in detail including *RNR3* (32,33), *FLO1* (34), *ANB1* (35), *SUC2* (36,37) and other a-cell-specific genes (38–40). Tup1-dependent nucleosome positioning at the promoter regions of these genes is believed to repress transcription by limiting the accessibility of promoter elements to *trans*-acting factors (26).

In this study, we defined the genomic landscape for Tup1's regulation of chromatin structure, mapping chromatin in both wild-type and *tup1Δ* cells using a combination of matched micrococcal nuclease (MNase) digestions and high-throughput DNA sequencing methods. We identified Tup1-specific alterations in chromatin architecture at 96 genes across the genome and determined that Tup1 stabilized the positioning of the −1 and −2 promoter nucleosomes of these genes when Tup1 is actively repressing transcription. We determined that Tup1 regulates chromatin organization at the majority of its targets by cooperation with the ATP-dependent chromatin remodeler Isw2. In addition, we also identified distinct chromatin architecture at Tup1-bound promoters consisting of a wide NDR with low occupancy/poorly positioned promoter nucleosomes, and a larger number and wider distribution of transcription factor-binding sites (TFBS). These distinctive Tup1-bound promoters regulate genes which have high transcription plasticity, suggesting a functional role for the Tup1–Ssn6 complex in regulating genes with varied expression.

MATERIALS AND METHODS

Yeast strains and growth conditions

Wild-type (BY4741) and *tup1Δ* (BY4741/*tup1Δ::*KanMX) strains (Open Biosystems) were used for nucleosome mapping experiments. Tup1 deletion was confirmed by PCR analysis of genomic DNA. Chromatin mapping experiments sampled from the genomes of yeast strains growing at 30°C in exponential phase (0.6–0.8 OD_{600}), as described previously (41).

Analysis of Tup1 ChIP-chip data

To compare low-resolution (0.5–1 kb) ChIP-chip experiments of *Hanlon et al.* (42) to our high-resolution nucleosome mapping data, ChIP-chip data were converted into a continuous binding profile. Both continuous binding ($\log_2$ ratio) and *P*-value profiles were generated by ChIPOTle's sliding window approach (43). The probability of Tup1 binding to any gene's regulatory region was assigned as the minimal *P*-value for the ChIPOTle windows overlapping that region. In this approach, every gene is assigned a *P*-value for Tup1 binding. Regulatory regions with a Bonferroni corrected $P < 1 \times 10^{-6}$ and mock uncorrected $P > 0.001$ in any growth condition were designated as strongly bound. Weakly bound regions were also selected as regions with a Boniforroni corrected $P < 1 \times 10^{-3}$ and mock uncorrected $P > 0.001$ (Table 1).

Matched MNase digestions

Preparation of chromatin DNA samples for sequencing was conducted as described previously (16,25,44), with several key revisions (Supplementary Figure S1A). Cross-linked chromatin–DNA complexes were extracted by mechanical disruption (bead beating; 4×1 min sessions, 2 min on ice between sessions). MNase titrations were carried out as described previously (25); however, an added level of standardization was achieved by quantifying the input of extracted chromatin loaded into each digest reaction; 1 mg total protein from whole-cell extracts per 200 µl digest reaction. Total protein concentration for whole cell extracts (chromatin extracts) was quantified using a Bradford assay (OD_{595}). Following MNase treatment and cross-link reversal, DNA was phenol:chloroform precipitated, resuspended in 50 µl TE pH 8.0, and RNase treated. Small aliquots (20%, ~10 µl) from each digest titration were then analyzed by gel electrophoresis (Supplementary Figure S1B). Gel intensity measurements for each lane were calculated using standard densitometry software provided by Biorad (Quantity One™) and exported to Microsoft Excel™ for correlation analysis (Pearson). Correlation coefficients were

Table 1. Tup1 binding at yeast regulatory regions

Regulatory region	Abbreviation	ChIPOTle, *P*-value*	No.
Not bound	NB	>0.001	5323
Strongly bound unidirectional	SBU	<0.000001	238
Weakly bound unidirectional	WBU	<0.001	189
Strongly bound bidirectional	SBB	<0.000001	160
Weakly bound bidirectional	WBB	<0.001	74
Unknown	Unk	NA	379

*ChIPOTle *P*-values are corrected for multiple testing. Unknown is caused by bad IP data.

calculated for digest titration levels no longer showing a visible di-nucleosome band (i.e. optimally digested samples) and spanning a region known to cover a size range of 0–400 bp of DNA (Supplementary Figure S1C). A 100-bp standard ladder (Qiagen) was analyzed on the same gel to calculate a relative front (i.e. separation relative to standard fragment sizes) for the migrating DNA population. 'Matched' digests were selected as two optimally digested samples having a correlation coefficient ($r > 0.9$). Correlation coefficients $r > 0.9$ were selected because these showed the most reproducible change in MNase protection data on single site real-time quantitative PCR (RT-qPCR) analysis (See Supplementary Methods section). The remaining sample from each optimal digest was column purified (Zymo Research), bypassing the need to gel excise mono-nucleosome DNA. Avoidance of gel extraction to isolate chromatin DNA at this stage is a key step to assure sampling of similar chromatin populations. Matched DNA samples were prepared for sequencing using the standard Illumina protocol with additional care at the gel purification step to ensure that the same size range of DNA was selected.

Nucleosome mapping

Nucleosome DNA was sequenced by an Illumina Genome Analyzer IIx, as described previously (16,25,45). Sequencing reads were aligned to the March 2010 build of the *S. cerevisiae* genome (www.yeastgenome.org) using the ELAND algorithm, allowing only two possible mismatches. MNase protection was calculated for sequencing data and all comparison data sets by extending aligned reads by 120 bp, dividing by the average read count per base pair and converting this ratio into continuous space ($\log_2$ ratio). Each data set was then standardized at single base pair resolution to have a mean occupancy of 0 and a standard deviation of 1. Individual nucleosome calls were made using the template filtering algorithm with default parameters, the seven standard defined templates and a minimum and maximum allowable nucleosome width of 80 and 220 bp, respectively (25).

Nucleosome statistics

Transcription start-site aligned data comparisons. Yeast transcription start sites (TSSs) were taken from *David et al.* (46). Significant differences for Tup1-bound and unbound promoters between wild-type and *tup1Δ* average MNase protection plots were tested at 10-bp resolution for regulatory regions spanning TSS (−1000 to +200 bp) using a two-tailed *t*-test. The resulting *P*-values were corrected for multiple comparisons by conservative Bonferroni correction. Tup1-bound promoters were sorted by downstream expression changes following Tup1 deletion using data from Green *et al.* (28). Genes with decreased downstream gene expression following Tup1 deletion were selected as being in the bottom 15% (15th percentile) of genes expressed in *tup1*Δ. Likewise, genes with increased downstream gene expression following Tup1 deletion were selected as being in the top 15% (85th percentile) of genes expressed in *tup1*Δ.

Template filtering comparisons. Nucleosomes called by template filtering were annotated to their closest promoter according to distance from TSS. The closest nucleosome upstream of each TSS, dyad within 500 bp, was annotated as −1, with the second closest as −2, and third as −3. Similar annotations were made for downstream +1, +2 and +3 nucleosomes, respectively, for each promoter. Comparisons between called nucleosomes from unbound (Class NB) versus bound (Class SBU) promoters were made using 10 000 permutation tests. Permutation testing randomly sampled the unbound promoter nucleosome data set for the parameters under examination. A similar analysis was conducted when comparing bound/wild-type versus bound/*tup1Δ* promoter nucleosomes.

RESULTS

Matched MNase digests produce highly correlated chromatin samples

To dissect the influence of Tup1 on chromatin structure *in vivo*, we employed a technical approach which minimizes the technical variation typically associated with MNase digestion steps utilized by genome-wide chromatin DNA preparations (see 'Materials and Methods' section; Supplementary Figure S1A) (25). Our approach allowed us to systematically select similarly digested chromatin preparations (i.e. matched MNase digestions) to control for differences in nuclease digestion extent and collect highly comparable chromatin populations. Matched digests were collected, similar to other chromatin-mapping protocols, but with the addition of several key steps (See 'Materials and Methods' section) to help ensure greater consistency of DNA sampling. Overall nuclease digestion profiles were compared by analyzing chromatin DNA populations (i.e. DNA remaining following MNase treatment) separated by gel electrophoresis. Matched samples were selected as having a highly correlated ($r > 0.9$) distribution of chromatin DNA population size and abundance, as identified by ethidium bromide DNA population staining intensities (Supplementary Figure S1B and S1C). Matched samples were then deeply sequenced in parallel using an Illumina Genome Analyzer IIx.

Sequencing of matched chromatin samples generated an extensive sequencing data set for the two strains with 20.6 and 23.7 million mapped sequencing reads for wild-type (BY4741) and *tup1Δ* genomes, respectively. Given that the yeast genome is packaged by an estimated 70 000 nucleosomes (47), our data represents greater than 250× average coverage for nucleosomal DNA. To our knowledge, the magnitude of this coverage provides the most extensive mononucleosome sequencing data set available for *S. cerevisiae* to date. Sequencing data was processed in three ways depending on the downstream analysis employed. First, we examined the ends of the sequence reads on individual strands (Figure 1A). This representation of the data is completely unprocessed and is an exact representation of the raw aligned sequencing output. Second, we extended each 36-bp sequence read to a total length of 120 bp. Although nucleosomes are 147 bp, we found that extrapolation to 120 bp provided better

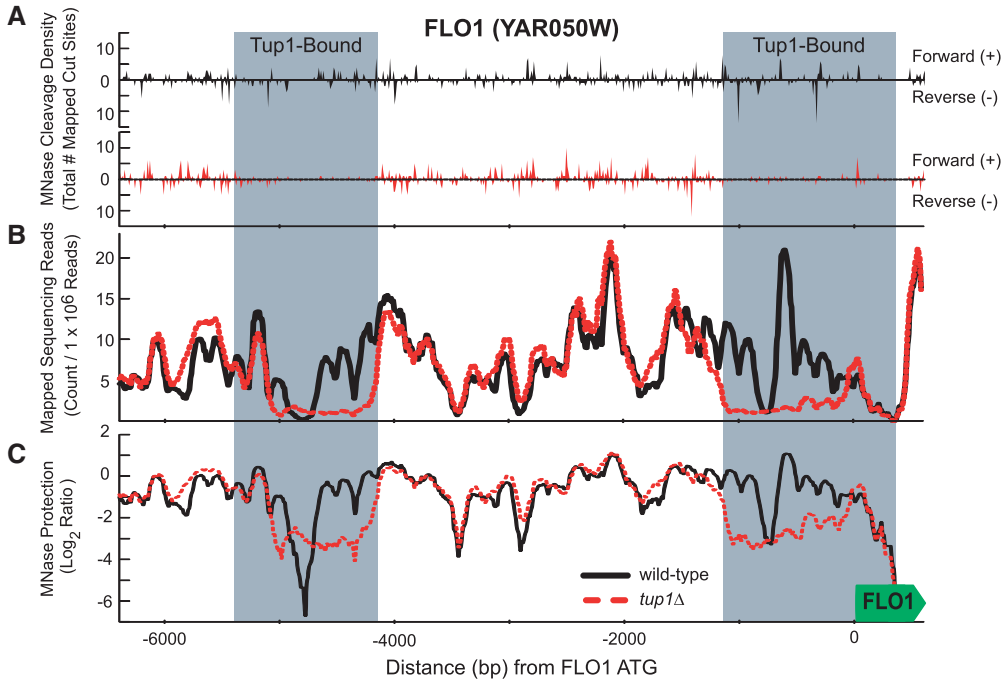

Figure 1. Matched MNase digests identify well-characterized Tup1-dependent changes in chromatin structure at the FLO1 promoter. Graphs illustrating sequencing data output, aligned to FLO1 ATG for wild-type (Black) and *tup1*Δ (Red) experiments. (**A**) Raw sequencing data output (MNase Cleavage Density) displaying the number of sequence read ends which map uniquely to the forward (upward scale) and reverse (downward scale) DNA strands. (**B**) Mapped sequencing reads are determined by extending the uniquely mapped tags to 120 bp and standardizing the total tag count to 1 million per experiment. (**C**) MNase Protection is the $\log_2$ ratio of the number of extended tags divided by the average read count per bp. Gray boxes: Regions of significant Tup1 enrichment by ChIP (Bonferroni corrected $P < 1 \times 10^{-6}$) (42).

demarcation of nucleosome ends than did extrapolation to 147 bp with no effect on occupancy comparisons. We then counted the number of times each unique position in the genome was included within a 120 bp extended sequence and standardized between experiments to a total of 1 million sequence reads, to correct for variable sequencing coverage (Figure 1B). Lastly, extended read counts were converted to a 'MNase protection' score by dividing by the average tag count per base pair, and converting into continuous data-space by calculating a $\log_2$ ratio (Figure 1C), similar to previous analysis (16,45). We prefer to use the term 'MNase protection' to describe this data rather than 'nucleosome occupancy' because MNase protection may alternatively be conferred by non-nucleosomal protein complexes. MNase protection reflects the relative level of DNA protection from MNase digestion and at most locations represent the occupancy/density of nucleosomes at each genomic location in relation to the entire genome sequenced in that chromatin preparation (48).

To test the homology between our two MNase protection data sets, a Pearson correlation coefficient was calculated comparing wild-type and *tup1Δ* chromatin maps across the entire genome. As expected, the correlations between our matched samples was extremely high ($r = 0.934$). To compare this homology to other data sets, the same correlation analysis was repeated for other published chromatin data sets of wild-type yeast of the same background genotype also grown in rich media. Across eight experiments from two different groups, only two experiments showed a correlation similar to ours (Supplementary Table S1). Interestingly, our matched samples, derived from different strains, were more similar than the majority of published replicates from the same strain. This result highlights how differences in technical preparation can introduce deviations into chromatin maps and how our matched preparation helps to control this influence.

To better visualize local versus global homology between our chromatin data sets, we calculated correlation coefficients and average changes in MNase protection for all 1-kb windows covering the yeast genome. As expected from our almost identical data sets, >90% of 1-kb windows had a correlation >0.9 and the majority of windows showed little change in average MNase protection (90% were within ±0.1) (Supplementary Figure S2). Overall, results from both approaches (correlation and average change) indicate that only a small fraction of the genome's chromatin changes in the absence of Tup1.

As an alternative approach to assess the similarity of our samples, we utilized a computational algorithm for characterizing nucleosome DNA signals from high-throughput DNA sequencing methods, known as template filtering (25). We employed this approach with the seven available templates to determine locations and characteristics for all nucleosomes in both data sets, mapping 57 469 and 57 327 nucleosomes each for wild-type and *tup1Δ* chromatin, respectively (Supplementary Table S2). Importantly, analysis of nucleosomes called by template filtering confirmed that wild-type and *tup1Δ* chromatin samples were of similar size populations and had similar

template frequencies, as expected of a matched digest (Supplementary Figure S3).

Importantly, our sequencing results also recapitulated results of published site-specific studies of nucleosome positioning at the PHO5 promoter (Supplementary Figure S4) (13). Nucleosomes at the PHO5 promoter have not been shown to be influenced by Tup1 regulatory mechanisms and, as expected, homologous levels of MNase protection are seen at this locus (between wild-type and *tup1*Δ chromatin) compared to known Tup1-regulated regions including FLO1, SUC2 and RNR3, which showed significant dissimilarity that was specific to the loss of Tup1 (See next section).

Matched MNase digests identify Tup1-specific differences in chromatin structure

Having successfully prepared highly correlated chromatin data sets, we hypothesized that the high degree of homology between our samples would enhance our ability of detecting Tup1-specific differences in chromatin structure, when comparing our wild-type and *tup1*Δ data sets. To test this hypothesis, we explored the relationship between Tup1 binding and chromatin structure differences between our data sets by integrating our sequencing data with a recently published ChIP-chip data set on Tup1 binding (42). Specific genomic fragments were scored for Tup1 binding with a *P*-value and/or Tup1 occupancy (binding) score (see 'Materials and Methods' section). Depending on the analysis, 100-bp genomic segments or 1-kb regulatory regions were scored. A gene's regulatory region was defined as extending 1-kb upstream of the open reading frame, and each such regulatory region was classified with respect to Tup1 binding by *P*-value (Table 1). Each bound regulatory region was further classified as bidirectional or unidirectional depending on if it was upstream of two divergently transcribed genes (list of all regulatory regions available in Supplementary Table S3). For the majority of our analysis, we compared regulatory regions classified as not bound by Tup1 (NB) to strongly bound unidirectional (SBU) and/or weakly bound unidirectional (WBU) (Table 1). Importantly, integration of genome-wide Tup1-binding data with our chromatin sequencing data sets revealed that our approach accurately reproduced the results of many high-resolution single-site studies on the perturbation of chromatin by Tup1. For example, at the well-studied Tup1-regulated locus, FLO1, peaks of Tup1 enrichment aligned with close proximity to regions of chromatin dissimilarity between matched-digest wild-type and *tup1Δ* samples, consistent with the effects of a known direct-acting Tup1–Ssn6 repression mechanism at that location (Figure 1). Moreover, previously mapped differences in FLO1 chromatin structure between wild-type and *ssn6Δ* strains were captured by our analysis with high fidelity and sensitivity, including changes in nucleosome occupancy and positioning directly upstream from transcription start (−1000 to −1 bp) and long-range differences (−5000 to −4000 bp) (34). In addition to FLO1, the well-documented role of Tup1 in establishing nucleosome positioning and occupancy at the SUC2 and RNR3 promoters was also evident in our data (Supplementary Figure S5 and S6) (32,33).

To examine our MNase protection data genome-wide in relation to Tup1 binding, we plotted the MNase protection profiles (i.e. nucleosome occupancy) for both data sets against each other for consecutive non-overlapping 100-bp windows covering the entire yeast genome (Figure 2A). As expected from the high correlation coefficient for our data sets, the plot illustrated clearly that the majority of the genome's 100-bp segments maintained similar MNase protection values regardless of the presence of Tup1 ($R^2 = 0.86$). Interestingly, however, regions with dissimilar MNase protection profiles between wild-type and *tup1Δ* data sets occurred in a directional fashion, whereby decreased nuclease protection was only seen for *tup1Δ* data relative to wild-type. The loss of MNase protection (and underlying nucleosome occupancy) when Tup1 is deleted is consistent with Tup1–Ssn6's role in stabilizing nucleosomes *in vivo* (26) (41). The specificity of this result can be discerned when plotting only regions of the genome containing the lowest Tup1-binding scores (Bottom 10%) and comparing to regions with the highest Tup1-binding scores (Top 10%) (Figure 2B and C, respectively). When the bottom 10% of Tup1-binding sites are plotted there is an absence of locations showing a loss in MNase protection when Tup1 is deleted, and the similarity between chromatin data sets improves ($R^2 = 0.92$). On the other hand, when examining the top 10% of Tup1-binding sites there is a large directional bulge and the chromatin data sets show increased dissimilarity ($R^2 = 0.72$). These data demonstrate that differences in MNase protection between our chromatin data sets, across the yeast genome, are specifically related to neighboring Tup1 binding and occur in a directional fashion consistent with Tup1's role in stabilizing nucleosome occupancy. It is important to remember that the Tup1 ChIP-chip data were obtained at low resolution (0.5–1 kb), and many of the sites with high Tup1-binding scores would be caused by proximity to true binding locations. Given this difference in resolution, it is likely that the specificity of the plot in Figure 2C is underestimated.

As an alternative approach to investigating the specificity of Tup1 binding to chromatin structure differences between our data sets, regions of chromatin dissimilarity (1-kb windows or larger) were classified as either having a poor correlation between MNase protection data ($r < 0.5$) or a large average change in MNase protection across a given region of interest (*tupΔ*-wt < -0.5). The average Tup1-binding score was calculated for these dissimilar regions and compared to a random sampling of similar-sized windows across the yeast genome (Figure 2D and E). Overall, regions of high dissimilarity in chromatin structure were enriched for Tup1 binding to a significantly greater extent than randomly sampled regions, indicating that high Tup1 enrichment was a specific characteristic of dissimilar chromatin regions between our data sets, again consistent with Tup1's role in modifying chromatin structure (26). Interestingly, the specificity of Tup1 enrichment to chromatin dissimilarity between wild-type and *tup1Δ* data sets was eroded when unmatched wild-type chromatin preparations were instead compared to our *tup1Δ* data

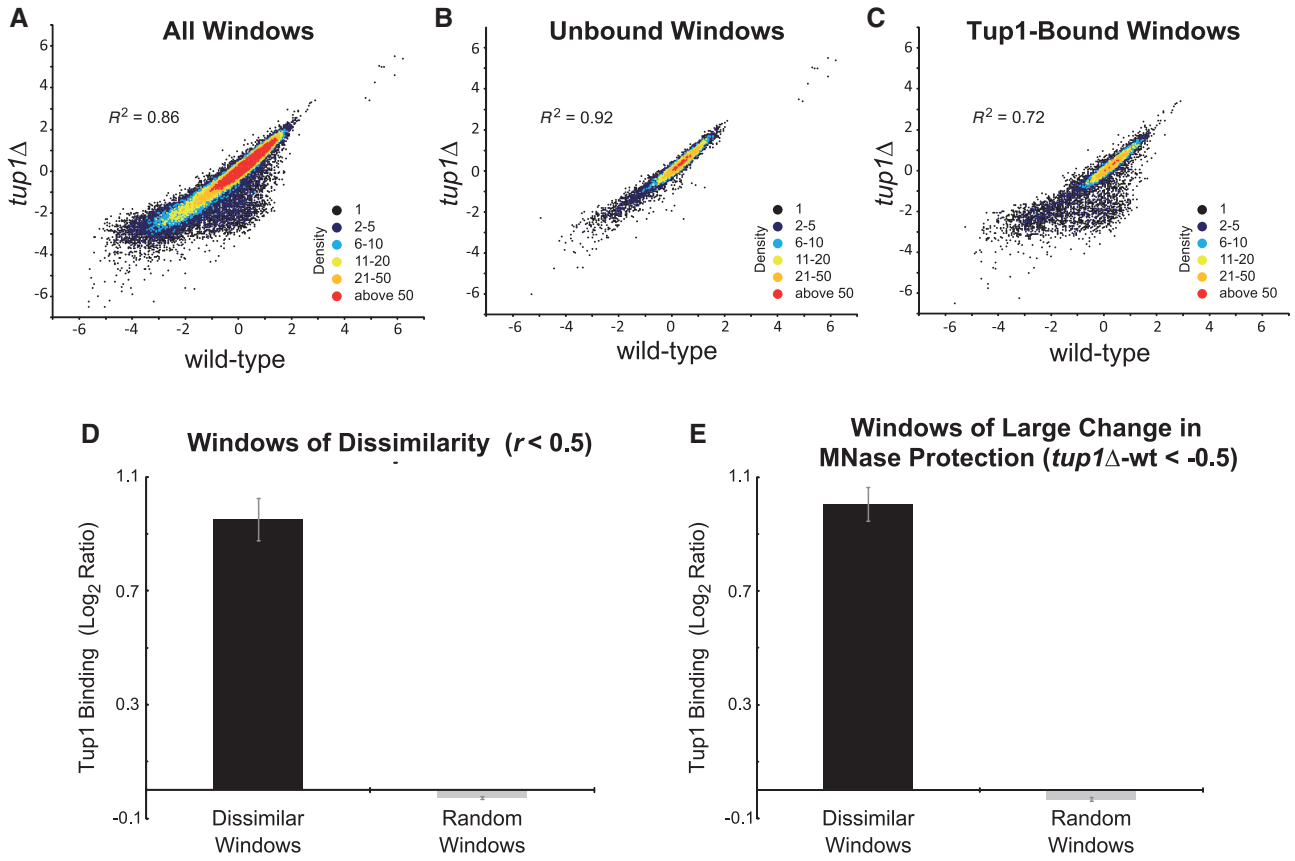

Figure 2. Deletion of Tup1 causes a loss in MNase protection at Tup1-bound sites. (**A**) Density plot displaying MNase protection profiles for wild-type versus *tup1*Δ data sets for all non-overlapping 100-bp segments spanning the entire yeast genome. (**B**) Density plot of 100-bp genome segments in *2A* which are not bound by Tup1 [bottom 10% enrichment by ChIP (42)] (**C**) Density plot of 100-bp genome segments in *2A* that are bound by Tup1 [top 10% enrichment by ChIP (42)]. (**D**) Average Tup1 binding ($\log_2$ ratio calculated from ChIP enrichment score, see 'Materials and Methods' section) seen at dissimilar regions, identified by correlation between wild-type and *tup1*Δ chromatin structures (Black bar) compared to Tup1 enrichment seen at randomly sampled (n = 10 000) genomic regions (Gray bar). Randomly sampled windows were composed of an identical window size composition to the dissimilar regions. Error bars represent standard error in average Tup1-binding scores across sampled windows. Dissimilar regions were defined as continuous windows (≥1 kb) with a correlation $r < 0.5$ between the data sets. (**E**) Same analysis as 2D for regions (≥1 kb) with a large average change in MNase protection between chromatin structures (*tup1*Δ–wt < -0.5) compared to randomly sampled (n = 10 000) genomic regions, again with an identical window size composition.

(Supplementary Figure S7). The decrease in average Tup1 enrichment seen at regions of dissimilarity between wild-type and *tup1Δ* chromatin structures when unmatched chromatin samples are compared highlights the utility of collecting highly correlated chromatin DNA populations.

Tup1 primarily influences chromatin structure at promoter regions

Comparing wild-type and *tup1Δ* chromatin maps allowed us to dissect the genomic landscape of Tup1's influence on chromatin structure. In total, the dissimilar windows identified by analysis for Figure 2D and E cover <4% of the budding yeast genome sequence, consistent with Tup1's presumed role modifying select regions of chromatin, rather than more broadly perturbing the genome at-large. Of dissimilar regions, 78% of dissimilar regions were identified by both correlation and average change analysis, suggesting that the loss of Tup1 regulation influences both nucleosome occupancy and positioning *in vivo*.

Localization of Tup1–Ssn6 is known to vary from gene to gene and its influence on chromatin structure has been documented at both intergenic regions and overlying coding sequences (26). Of the 238 unidirectional regulatory regions bound strongly by Tup1 (Class SBU) in our experiments, 92 (38.7%) were identified as having at least 500 bp of dissimilarity (by correlation, average change, or both) between wild-type and *tup1Δ* with 31 (13%) coding regions identified as being dissimilar. In total, 14 of the 31 dissimilar coding regions identified were also associated with a dissimilar regulatory region, indicating that Tup1's activity on chromatin structure is predominantly based at promoter regions, a feature seen throughout our analysis.

Tup1-bound genes show a distinct open chromatin architecture at promoter regions

To assess differences in promoter packaging within and between our chromatin data sets, genes were aligned by TSS and averaged MNase protection was plotted at 10-bp

resolution for a 1-kb window up and downstream of the TSS, similar to previous studies (16,45). As expected, average aligned MNase protection data were extremely similar between wild-type and *tup1Δ* strains for all yeast TSS overall (Figure 3A). Like typical yeast promoters, both wild-type and *tup1Δ* averaged MNase protection (nucleosome occupancy) plots displayed a NDR directly upstream of the TSS flanked by well-positioned nucleosomes, especially over the coding region. The same characteristic pattern of MNase protection was also seen for all promoters not bound by Tup1 (Figure 3B). However, when promoters bound by Tup1 were examined alone, a markedly different pattern of chromatin structure was seen. As illustrated by Figure 3C, genes with promoters bound by Tup1 (Class SBU) exhibited an increased NDR width upstream of the TSS, and a significantly different pattern of nucleosome occupancy and positioning surrounded that region compared to unbound (Class NB) promoters (Figure 3B). The unique chromatin structure profile associated with Tup1-occupied promoters was not a product of our data normalization and transformation procedures, since the same result was seen when our data was viewed in non-continuous count space (Supplementary Figure SF8).

As an alternate analysis of promoter structures, we also analyzed our chromatin data by individually calling

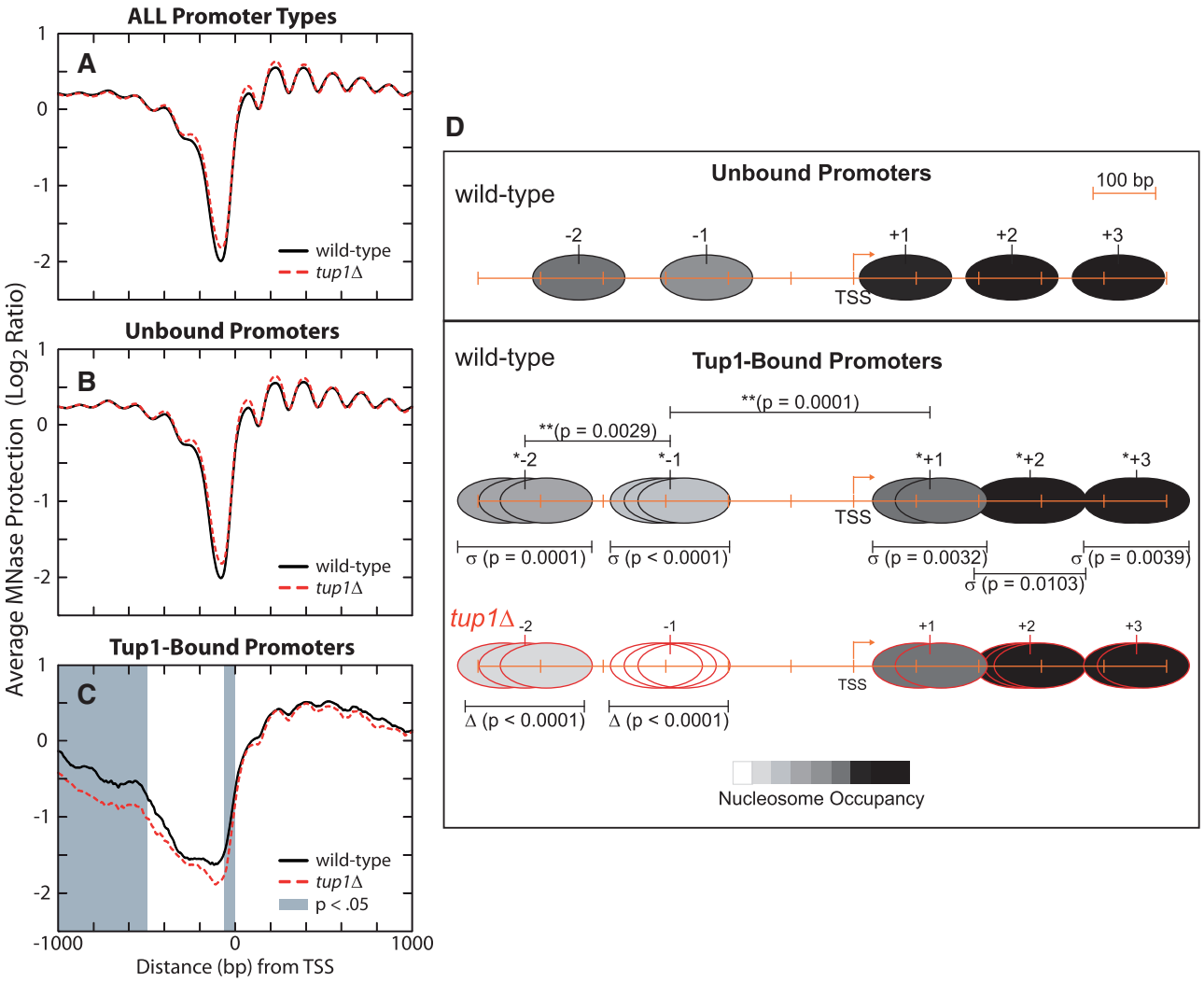

Figure 3. Tup1-regulated promoters have a more open chromatin structure compared to the rest of the yeast genome. (A–C) Graphs of average MNase protection profiles aligned by TSS and sorted into specific promoter classes (Table 1) for wild-type (Black) and *tup1*Δ (Red) data sets. Only genes with mapped TSS are shown (46). (**A**) Average profiles for all promoter types listed in Table 1, excluding those of unknown type ($n = 4741$) (**B**) Average profiles for unbound promoters (Class NB; $n = 4298$). (**C**) Average profiles for Tup1 unidirectional-bound promoters (Class SBU; $n = 162$). Gray boxes: Regions of significant change in average MNase protection following Tup1 deletion, as determined by two-tailed *t*-testing (Bonferroni corrected $P < 0.05$). (**D**) Figure drawn to scale, depicting promoter nucleosomes for wild-type (Black ovals) and *tup1Δ* (Red ovals) chromatin data sets. Promoter nucleosome statistics were calculated for nucleosomes called by the template filtering algorithm (25) and annotated to individual promoters as described in 'Materials and Methods' section. Relative nucleosome occupancy (density at each locus) is represented by shading inside nucleosomes (White = low, Black = high). Asterisks (*) denote significant decrease in nucleosome occupancy compared to unbound promoters. Double asterisks denotes significant increase in distance (bp DNA) compared to unbound promoters. Sigma denotes significant increase in the variability of nucleosome positioning (i.e. the standard deviation for called nucleosomes dyad locations) compared to unbound promoters. Open triangle denotes a significant loss in nucleosomes called by template filtering compared to wild-type Tup1-bound promoters (Class SBU).

promoter nucleosomes using template filtering (25). This analysis revealed that the −2, −1, +1, +2 and +3 promoter nucleosomes all showed significantly lower nucleosome occupancy values and significantly more deviance in positioning at Tup1-bound promoters, compared to their unbound counterparts (Figure 3D). As suggested by the broader NDR, the internucleosomal distance between the −1 and +1 nucleosomes was significantly larger (40-bp increase; $P = 0.0001$). Additionally, a significantly increased inter-nucleosomal distance between the −1 and −2 nucleosomes (29-bp increase, $P = 0.0029$) was also evident compared to unbound promoters. Distances between +1, +2 and +3 nucleosomes remained unchanged.

In addition to examining our MNase protection data in relation to Tup1 binding, we also preformed unsupervised clustering to categorize promoters across the genome in relation to our two data sets (Supplementary Figure S9). *K*-medoids clustering with values of $K > 3$ consistently produced a discrete cluster with a wide NDR region, similar to that seen for Tup1-bound promoters in Figure 3C. Hypergeometric distribution analysis for this wide-NDR cluster consistently revealed an enrichment for Tup1-bound promoters and also enriched for promoters with a GO Slim annotation for genes involved in translation. These results suggest a possible link between the wide NDR structure we are seeing, Tup1 binding, and specific biological pathways.

Tup1-bound promoters are accessed by more transcription factors which bind across a wider region

Having characterized a distinct chromatin structure associated with Tup1-bound promoters, we next sought to identify additional mechanisms that could best explain the observed pattern of MNase protection (and underlying nucleosome positioning/ occupancy) at these loci. Previous work has shown that both TFBS locations and active (occupied) binding sites *in vivo* are preferentially enriched at the characteristic NDR region upstream from each promoter's TSS, consistent with the model that nucleosome occupancy has a strong influence on transcription factor (TF) occupancy (49–53). Given these characteristic distributions and their relationship to chromatin structure at promoter regions, we tested whether differences in TFBS locations underscored the distinct chromatin structure profiles associated with Tup1-bound and unbound promoters. Using the locations of highly conserved TFBSs identified by *MacIsacc et al.* (51), we plotted the distribution of conserved TFBS locations in relation to downstream-coding regions (ATG) and overlying chromatin data (Figure 4A and B). As illustrated by Figure 4A and B, promoters not bound by Tup1 showed a characteristic distribution of TFBS locations, with locations correlating to overlying occupancy profiles and significantly enriching at the characteristic NDR region (−10- to −200-bp upstream of ATG) upstream of coding regions, similar to previous analysis (49). In contrast, Tup1-bound promoters showed a wider distribution of conserved TFBS locations, lacking the peak of enrichment of TFBS locations at the characteristic NDR region (−100 to −200 bp). Conserved TFBS locations at Tup1 promoters were instead more spread out in their distribution across the promoter region, consistent with the distinct wide-NDR architecture of these genes. Importantly, the unique distribution of TFBS locations was also seen for conserved TFBSs active in the condition tested (bound in YPD), was observed when compared to wide unbound promoters, and was not dependent on promoter type (single versus double) or Tup1-binding class (Data not shown).

Knowing that sequence-specific DNA-binding TFs must compete with and/or interact with nucleosomes to bind DNA and regulate transcription, we hypothesized that an increased number of TFs and/or TFBSs could be present at Tup1-bound promoters, either causing or resulting from the unique chromatin architecture and underlying TFBS distributions we identified. To test this hypothesis, we calculated the average number of conserved TFBSs and TFs present for each promoter class in Table 1. As illustrated by Figure 4C and D, Tup1-bound promoters showed a significantly larger number of both conserved TFBSs and bound TFs compared to unbound promoters, on average. Importantly, significant differences were seen regardless of Tup1-binding class and an even larger difference was evident for both TFBS number and number of bound TFs when we compared Tup1-bound single promoters versus unbound single promoters (data not shown).

Tup1-regulated genes are more plastic in downstream expression

Having uncovered a distinct structure for Tup1-bound genes, we hypothesized that the wider NDR with the higher number and spreading of conserved TFBSs would allow Tup1-regulated genes to respond more readily to various environmental signals. Accordingly, we proposed that Tup1 binding would be associated with the capacity to modulate gene expression upon changing environmental conditions, i.e. transcriptional plasticity (54). To examine transcriptional plasticity we used an extensive microarray data set for yeast grown in 13 diverse environmental transitions (55) and calculated transcriptional plasticity as the standard deviation for a gene's expression across all growth conditions. As illustrated in Figure 5A, our analysis found that Tup1 binding was significantly correlated ($P = 4.0 \times 10^{-55}$) to transcriptional plasticity. Importantly, we also tested the specificity of the relationship between Tup1 binding and downstream expression plasticity by conducting the same analysis for all regulatory factors bound in rich media. Interestingly, we found that the association of Tup1-binding with downstream plasticity is stronger than that seen for all other factors tested, implying that plastic gene expression is a specific property of Tup1-regulated genes (Figure 5B). Overall, the strong association of Tup1 binding with downstream expression plasticity suggests that the distinctive packaging of Tup1-bound promoters may reflect a shared ability to broadly alter gene expression programs via Tup1 regulation to coordinate appropriate responses to environmental signals.

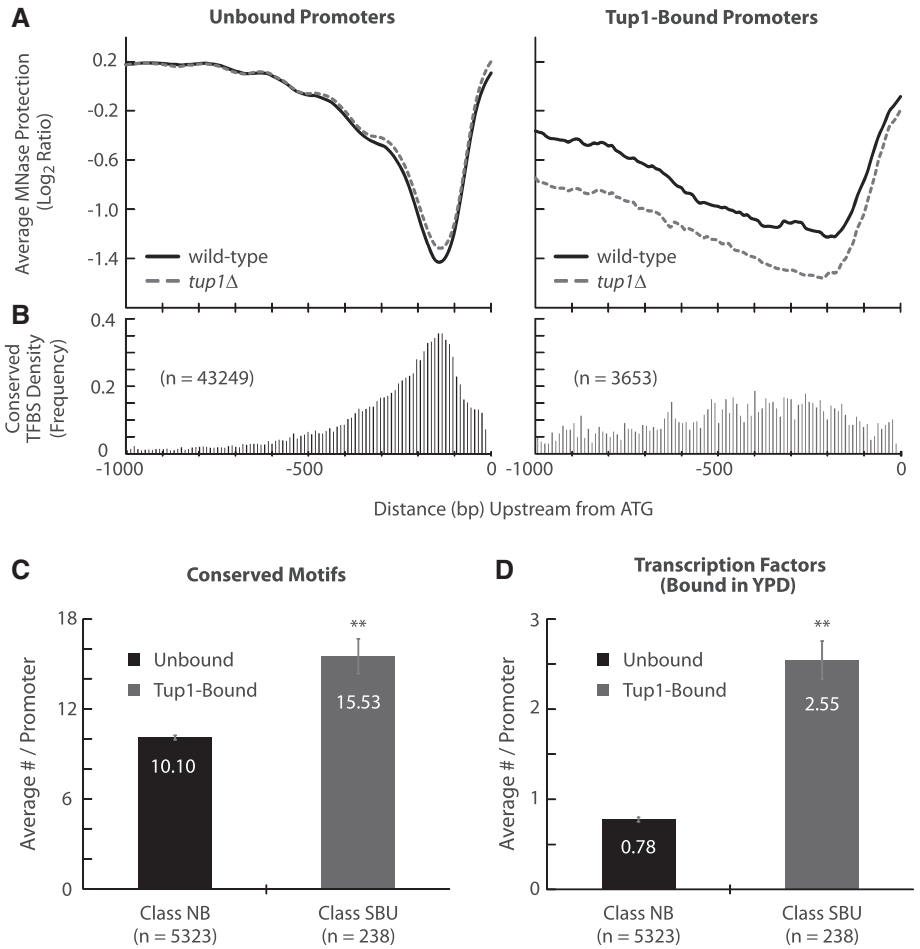

Figure 4. Tup1-bound promoters show a unique distribution of TFBSs and are targeted by more transcription factors than unbound promoter regions. (**A**) Comparison of average MNase protection profiles (i.e. nucleosome occupancy) and (**B**) the underlying distribution of conserved TFBS locations at unbound (Class NB) and Tup1-bound (Class SBU) promoters, aligned by ATG. Data was plotted relative to translation start rather than transcription start due to the larger number of available TFBS locations and chromatin data using this approach. (**C**) Comparison of the average number of conserved TFBSs present at unbound promoters (Class NB) compared to Tup1-bound (Class SBU) promoters. (**D**) Comparison of the average number of TFs bound at unbound promoters (Class NB) compared to Tup1-bound (Class SBU) promoters. Double asterisks denotes a statistically significant increase ($P < 0.0001$) for (C) and (D). Error bars represent standard error in average signal detection.

Tup1 stabilizes the −1 and −2 promoter nucleosomes

Having identified several structural features unique to Tup1-bound promoters, we next sought to examine how the deletion of Tup1 influenced this chromatin structure, hoping to cast light onto the mechanism by which Tup1 regulates chromatin. Analysis of our TSS plot of Tup1-bound promoters (Figure 3C) revealed that deletion of Tup1 caused a decrease in MNase protection across the entire intergenic region with significant decreases at −1000 to −450-bp upstream of the TSS and directly upstream of the TSS; −70 to −10 bp (gray bars; Bonferroni corrected $P < 0.05$). Significant decreases in intergenic nuclease protection levels overlied the positions of the −2 and −1 promoter nucleosomes, upstream of the wider NDR, and suggest that Tup1-dependent nucleosome occupancy at these locations may play a key role in its regulatory mechanism. Additionally, when looking at individual nucleosomes called by template filtering, there was also a significant loss of called −1 and −2 promoter nucleosomes in the *tup1*Δ strain (Figure 3D).

Significant changes in the average MNase protection profile in Figure 3C may appear slight because this plot encompasses all Tup1-bound promoters, including loci where Tup1 is not regulating through chromatin. Therefore, to test the reproducibility of changes in MNase protection driving the significant differences identified in Figure 3C, changes in MNase protection and underlying histone H3 and H4 occupancy were assayed using RT-qPCR on three additional biological replicates at fifteen selected sites. As illustrated by Supplementary Figures SF10–SF12, strongly dissimilar regions between our data sets ($r < 0.5$; YMR319C, YLR295C, YBR157C) showed large reproducible changes in MNase protection on RT-qPCR analysis and weakly dissimilar regions ($0.5 < r < 0.7$; YIL056W) showed smaller changes also with high consistency. Importantly, changes in MNase protection were not seen

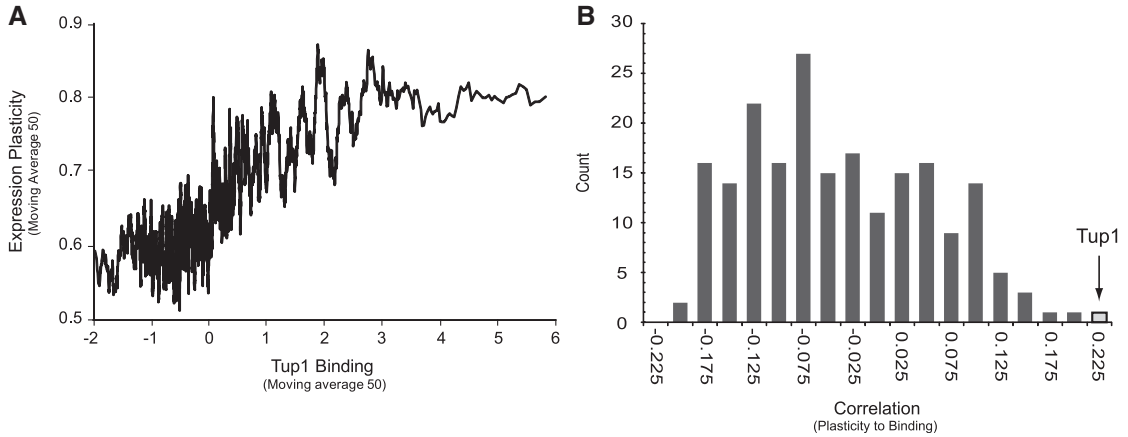

Figure 5. Tup1 binding at intergenic regions is specifically associated with transcription plasticity of downstream genes. (**A**) All genes for which there was data ($n = 5802$) have been sorted by Tup1 occupancy upstream (42) and the moving average (50 genes) for Tup1 occupancy versus expression plasticity is plotted. Expression plasticity was determined as the standard deviation across all 93 gene expression microarray experiments for various stress and metabolic responses (55). (**B**) Histogram displaying the correlation coefficients of genome-wide ChIP-chip data sets (204 proteins) versus expression plasticity (50,55). Tup1 (indicated by the arrow) has the highest correlation to expression plasticity ($r = 0.204$; $P = 4 \times 10^{-55}$).

at the well-characterized PHO5 locus, an expected result since this locus is not regulated by Tup1 (Supplementary Figure S10). Additionally, significant changes in nucleosome occupancy were also shown to underlie changes in nuclease protection profiles at all dissimilar regions tested thus demonstrating that at the majority of sites changes in MNase protection are caused by changes in nucleosome occupancy (Supplementary Figures S10–S12). Given these results, we were confident that strongly dissimilarity regions defined by an $r < 0.5$ were specific and reproducible, therefore, the remainder of our analysis focused on strongly dissimilar regions between our two data sets.

As an alternative approach to investigate Tup1 stabilization of promoter nucleosomes in relation to transcriptional regulation, we again performed an analysis of TSS-aligned data for Tup1-bound promoters, but additionally sorted the chromatin data into three groupings according to downstream expression in *tup1Δ* strains (28) (Figure 6A–C). Genes repressed by Tup1 and subsequently expressed (de-repressed) upon its deletion, again exhibited a similar decreases in MNase protection across the regulatory region, significantly at the location of the −2 nucleosome (Figure 6B, gray bars; Bonferroni corrected $P < 0.05$). Interestingly, an opposing result was obtained at genes where Tup1 may be playing a role in activation of expression (i.e. repressed in *tup1Δ*). In place of losing nuclease protection at activated promoters of these regions, we instead saw a slight increase in protection over the NDR region (Figure 6C), indicating that Tup1's influence on the chromatin at these regions is different from that at genes it actively represses. Additionally, when examining genes with expression profiles unchanged by Tup1 deletion in the condition being examined (rich medium; Figure 6A), no change in chromatin structure was seen, suggesting that the differences we see in chromatin structure for Tup1-bound genes are due to its role in repressing transcription.

In addition to sorting MNase protection data for Tup1-bound promoters by downstream expression, we clustered change in MNase protection profiles (*tup1*Δ—wt) for all Tup1-bound promoters for a 1-kb window surrounding TSS (Figure 6D). Clustering of bound promoters yielded only two significantly distinct patterns of change in MNase protection, regardless of the number of clusters generated. Cluster 1 had a broad increase in MNase protection across Tup1-bound promoters and consistently enriched for genes with associated GO slim process of translation, the same functional term associated with Tup1-bound promoters in our initial clustering analysis (Supplementary Figure S9). The broad increase in MNase protection seen at these promoters also parallels the increase seen for genes believed to be activated by Tup1 (Figure 6C). Cluster 2 showed a broad decrease in MNase protection across promoter regions and significantly enriched for downstream genes de-repressed in a *tup1*Δ strain, similar to the result in Figure 6B. The same changes in structural patterns for Tup1-bound genes were also seen when we clustered change in MNase protection data for all available TSSs (including unbound promoters). As illustrated in Supplementary Figure S13, broad increases or decreases in MNase protection are again seen for wide-NDR promoters that enrich for Tup1 binding (Clusters 1 and 2). Similar to results in Figure 6D–F, Tup1-associated promoters with a broad increase in MNase protection following deletion of Tup1 again enrich for genes associated with translation and ribosome biogenesis and assembly. In contrast, Tup1-associated promoters with a broad decrease in nucleosome occupancy following deletion of Tup1 enrich for genes involved in response to chemical stimuli and unknown biological processes. Together, results from Figure 6, Supplementary Figures S9 and S13 illustrate how Tup1 can have different effects on chromatin structure, depending on both the associated biological

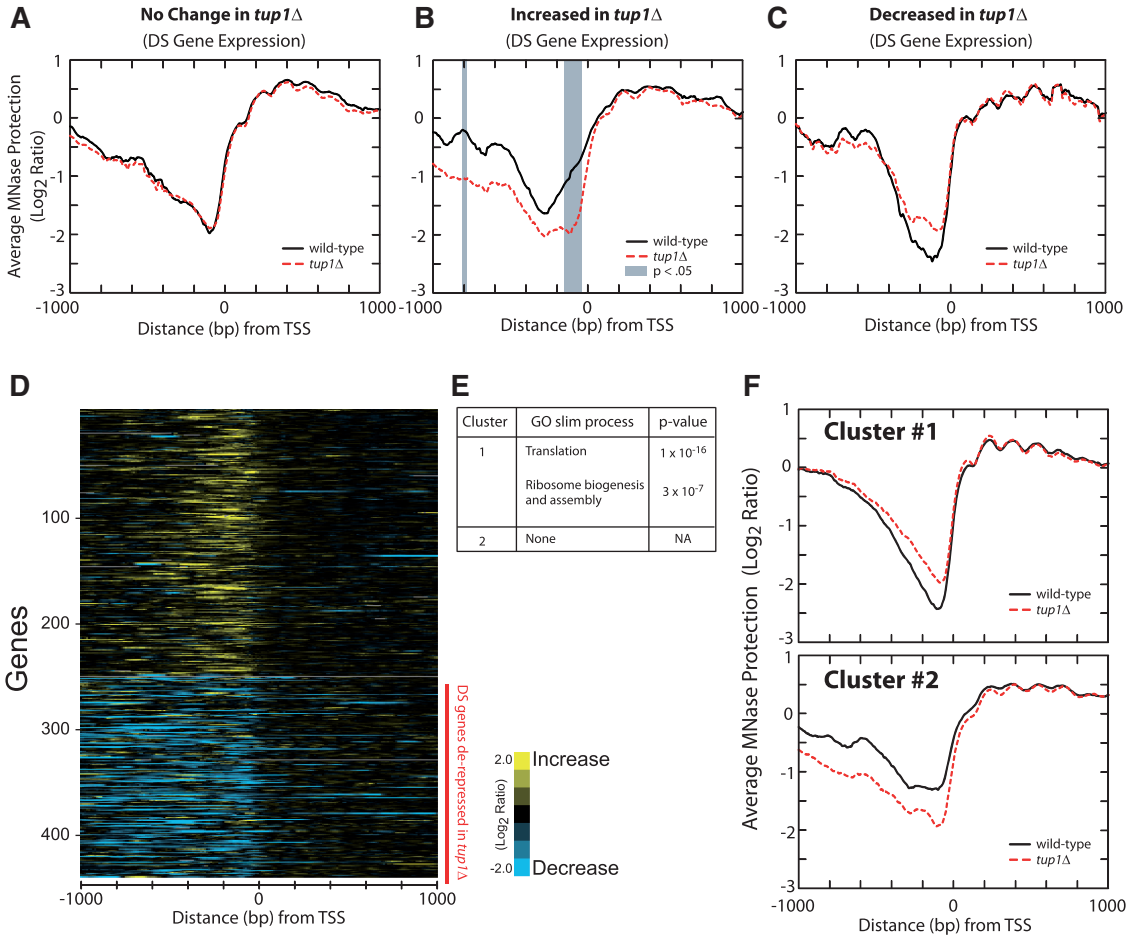

Figure 6. Tup1-dependent chromatin structure changes depending on the co-repressor's role in transcriptional regulation. (**A–C**) Graphs of the average MNase protection profiles for Tup1-bound promoters (Class SBU), sorted according to downstream expression changes following Tup1 deletion (see 'Materials and Methods' section) (28). Both wild-type (Black) and *tup1*Δ (Red) MNase protection data are plotted. Gray boxes: Regions of significant change in average MNase protection following Tup1 deletion, as determined by two-tailed *t*-testing (Bonferroni corrected $P < 0.05$). Only a few regions of repressed promoters demonstrated a significant loss of MNase protection because of the limited number of promoters in each category and the use of multiple testing corrections. For this analysis we tested a 1-kb region upstream of TSS (−1000 to 0 bp) at 10-bp resolution. DS = Downstream. (**D**) Heat map of relative changes in MNase protection data (*tup1*Δ–wt), aligned to TSS, for all Tup1-bound promoters (combining Class SBB, SBU, WBB and WBU). All four Tup1-bound promoter classes were included in this analysis to increase the number of promoters with available TSS for clustering. Change in protection data was clustered using unsupervised *k*-mediod clustering ($k = 2$) for data spanning 1-kb window up and downstream of TSS. (**E**) Table of statistically significant (Bonferroni corrected $P < 0.0001$) enrichments of GO Slim terms associated with genes in each defined cluster. Significant enrichments were identified by hypergeometric testing. (**F**) Graphical illustration of the average MNase protection data for each cluster. (Black) wild-type and (Red) *tup1*Δ data sets.

processes and downstream expression events involved at the genes it regulates.

Tup1 stabilizes nucleosomes at stress response TFBSs

Chromatin-dependent mechanisms of Tup1 repression are believed to repress transcription by limiting the accessibility of promoter elements to *trans*-acting factors (26). To explore the relationship between Tup1 regulation, chromatin structure and *trans*-activating factors, we examined the chromatin structure surrounding all annotated TFBSs (51). The average change in MNase protection (*tup1*Δ-wt) for each TF was determined, and change-in-protection data (*tup1*Δ-wt) were aligned by TFBS center. To identify relationships among the TFs, TFBS change-in-protection data were sorted by the average change-in-protection for the middle 100-bp centering on the TFBS (Figure 7A). Three distinct patterns of chromatin structure emerged (Figure 7B–D) whereby the average change in MNase protection profiles increased, decreased or did not change following Tup1 deletion (*tup1*Δ–wt). Overall, the majority of chromatin at TFBSs was not altered by Tup1 deletion, consistent with the fact that Tup1 regulates just a small fraction of the genome.

TFBSs which are centered on locations where MNase protection was decreased, suggesting nucleosome loss in a *tup1Δ,* could represent TFs whose binding is blocked directly by Tup1-stabilized nucleosomes or blocked by Tup1 itself. Indeed, several of the TFs (Mig1, Sko1, Nrg1, Phd1, Sut1, Aft1, Cin5, Skn7, Yap6, Rcs1, Rox1) that showed a dramatic loss of MNase protection in the *tup1Δ* strain were known co-factors of the Tup1–Ssn6

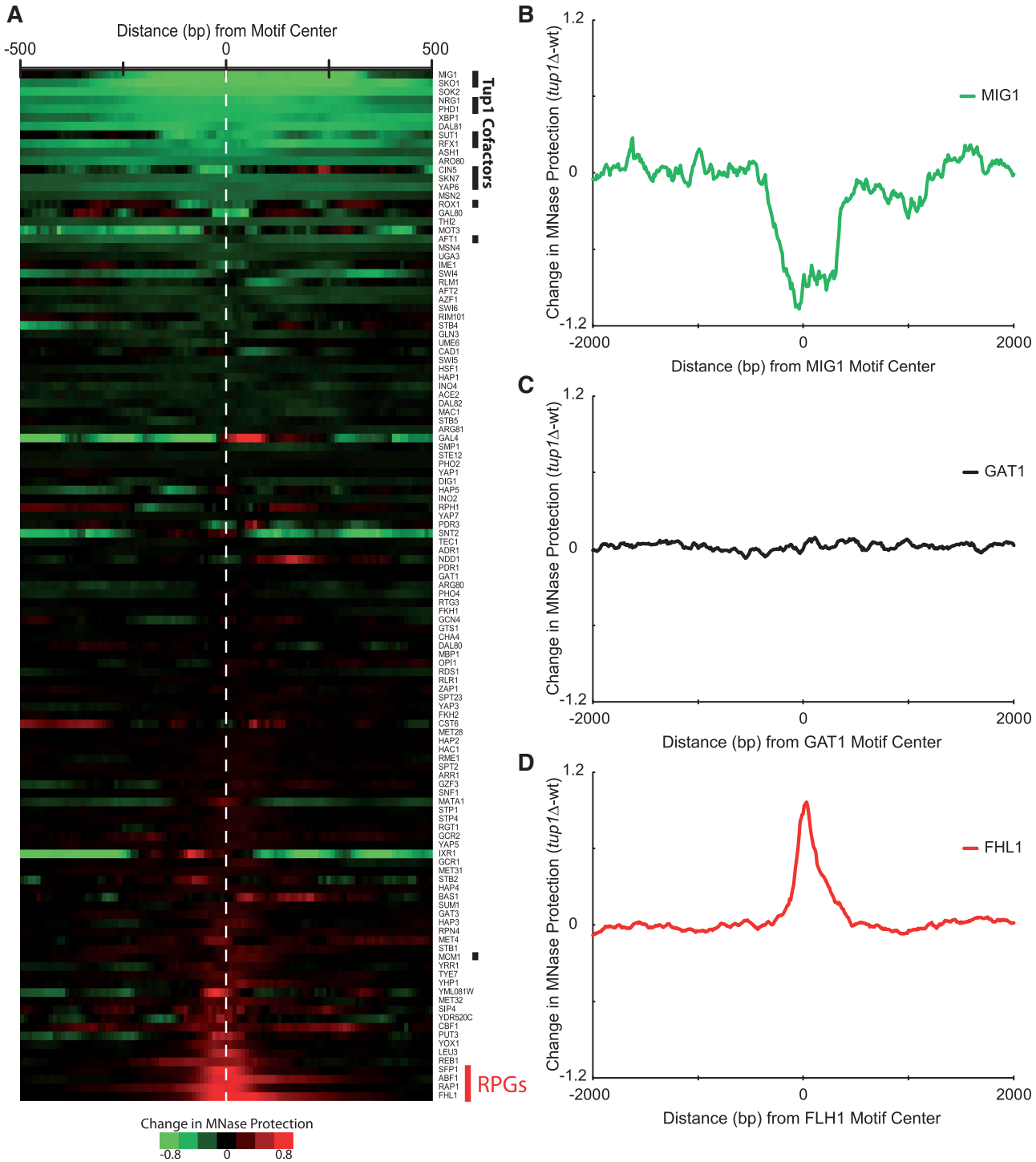

Figure 7. Tup1-dependent MNase protection overlies stress response factor binding sites, including many Tup1 recruiters. **(A)** Heat map of average change in MNase protection between chromatin data sets (*tup1*Δ—wild-type) from this study, centered on bound TFBSs (50,51). Occupancy data were sorted by average differences for a 100-bp window centered on TFBS. Black bars: known Tup1 recruiting factors. Red bar: Known regulators of ribosomal protein synthesis. **(B–D)** Curves showing the average change in MNase protection data (*tup1*Δ—wild-type) from this study for specific factors (MIG1—Green, GAT1—Black, FLH1—Red) representing the upper, middle, and lower percentiles of sorted data displayed in 7A.

complex. These TFs have been shown to physically interact with Tup1 or Ssn6 and are likely DNA-binding recruiting proteins for the Tup1–Ssn6 complex (42). Identification of these factors further confirms the specificity of our assay at detecting Tup1-specific changes in chromatin structure. Additionally, other TFs with TFBSs present at MNase protected regions dependent on Tup1 may represent still uncharacterized Tup1–Ssn6 cofactors or TFs whose binding may be regulated by Tup1. The general stress TFs Msn2 and Msn4 fall in this category and showed

decreased nuclease protection (i.e. nucleosome loss) in *tup1Δ*. Interestingly, Msn2/Msn4 have been shown to regulate many of the genes required for the environmental stress response (56–58), and our findings suggest that their binding may by regulated by Tup1-dependent nucleosome occupancy/positioning.

Surprisingly, there were a few TFBSs located at regions showing an increase in MNase protection following Tup1 deletion, including Rap1, Fhl1, Sfp1 and Abf1. All four of these TFs target protein biosynthesis genes, some of the most highly expressed genes in rapid growing yeast. Since Tup1 has been shown by ChIP-chip analysis to bind at many protein biosynthesis genes, this change in nuclease protection could be directly related to Tup1 regulation (42). To test if this increase in MNase protection was a direct or indirect effect of Tup1 regulation, we examined all genes annotated with the protein biosynthesis GO-slim term and compared between Tup1-bound and unbound regulatory regions (Supplementary Figure S14). Protein biosynthesis genes showed an increase of similar magnitude in MNase protection in the NDR upstream of the TSS, regardless of Tup1-binding class, suggesting that the change in MNase protection at these sites was not directly caused by Tup1. While this increase in MNase protection appears indirect, the overall architecture of Tup1-bound protein biosynthesis genes was significantly different from that of unbound protein biosynthesis genes. As we demonstrated earlier for all Tup1-bound genes, the NDR for Tup1-bound protein biosynthesis genes was significantly wider than for unbound protein biosynthesis genes and promoter nucleosomes showed variable positioning. This result suggests that there is a unique subset of protein biosysnthesis genes which is regulated by Tup1.

Isw2 remodels the majority of Tup1 remodeled chromatin

Having identified distinct effects of Tup1 on chromatin structure that relate to the associated biological processes and expression state of regulated genes, we next asked if Tup1's effect on chromatin structure was also associated with the activity of other regulatory factors. Tup1–Ssn6 has been shown to require the ATP-dependent chromatin remodeling enzyme Isw2 to position nucleosomes for gene repression at the well-characterized RNR3 locus, both upstream of and across the RNR3-coding region (32,33). Given the well-established collaboration between Isw2 and Tup1 nucleosome-positioning activities *in vivo* at RNR3 and the highly similar effects that Tup1 and Isw2 yield on upstream nucleosome occupancy (59–61), we hypothesized that the association of Isw2-remodeling with Tup1-remodeling events extended beyond individual loci and represented a more frequent collaboration of remodeling activities across the genome. To test this hypothesis, association testing was performed comparing Isw2-remodeled genes defined by *Whitehouse et al.* and Tup1-remodeled promoters identified by our analysis. Only 5′ Isw2 remodeling events were considered for this analysis, since the regions of significant Tup1 remodeling, we identified were at the 5′-end of genes (i.e. within 0- to −1000-bp upstream of TSS, Figure 3C). As illustrated in Figure 8A, a greater proportion of Tup1-remodeled sites were also remodeled by Isw2 (52%), when compared to non-Tup1-remodeled genes (21%). Importantly, with a relaxed stringency for defining Tup1 remodeling ($r < 0.7$) and inclusion of all Tup1-bound regulatory regions (SBU, WBU, SBB and WBB), there were a total of 96 Tup1 bound and remodeled genes of which 48 or 50% were also Isw2-remodeled. A significant association of Tup1 remodeling with Isw2 remodeling was also seen at unbound (Class NB) promoters and likely represent direct effects whose Tup1-binding state was not identified by previous low-resolution ChIP-chip experiments (42). Overall, the significant association of Tup1 remodeling with Isw2 remodeling indicates that collaborative actives of Tup1 and Isw2 seen at the RNR3 promoter extend beyond individual loci and represent a genome-wide regulatory collaboration.

Hypoacetylation of promoter histones is associated with active Tup1 repression

Decreased histone acetylation has been shown to track with Tup1–Ssn6 localization (62,63) and it is believed that Tup1 may repress gene expression by creating a self-reinforcing state through its interactions with hypoacetylated histones and histone deacetylase complexes (HDACs) *in vivo* (26,63–66). We hypothesized that Tup1 remodeling could be associated with a distinct histone modification profile at remodeled promoters, reflecting potential collaborative activities of Tup1 chromatin regulation with HDAC activity to regulate transcription. To test this hypothesis, we aligned average chromatin modification data from Pokholok *et al.* (67) for a 1-kb window surrounding TSS and compared modification profiles by Tup1-binding class. Interestingly, no significant differences in overall chromatin modification profiles were evident when comparing Tup1-bound promoters to unbound promoters (Figure 8B). Instead, only when Tup1-bound promoters were separated into Tup1 repressed genes versus non-repressed was hypoacetylation shown to track with Tup1 targets which are actively being repressed (Figure 8B). Additionally, a similar modification profile was also seen for Tup1-bound promoters that were either remodeled by Tup1 or remodeled by Isw2 (Supplementary Figure S15). This result suggests that Tup1's interactions with hypoacetylated histones and HDACs *in vivo* is a feature of actively repressed Tup1-bound loci and not Tup1 localization alone. Additionally, that the distinct chromatin modification profiles associated with gene repression mirrored those of Tup1- and Isw2-remodeled loci, further suggests that collaboration of HDAC complexes and other chromatin modifiers is a general feature of active Tup1 repression through chromatin.

DISCUSSION

Matched MNase digests reduce technical variation and reproducibly identify Tup1-specific changes in chromatin structure

Genome-wide chromatin DNA isolation protocols typically utilize a combination of nuclease digestion and gel electrophoresis to isolate mono-nucleosomal DNA

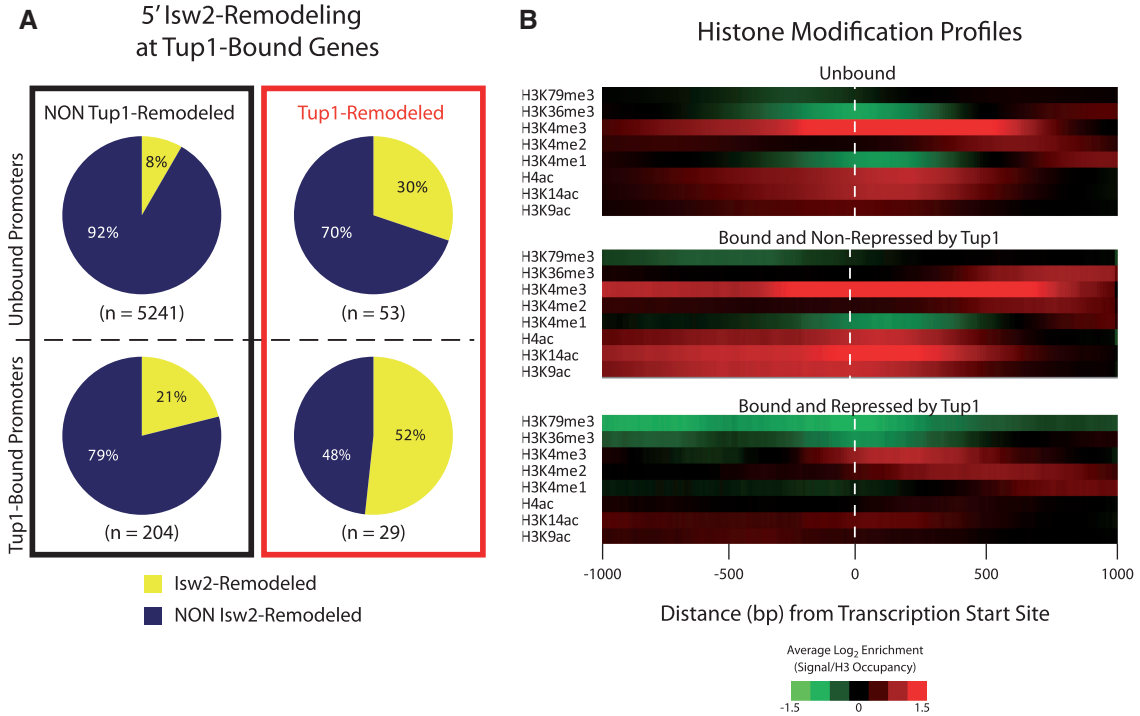

Figure 8. Chromatin remodeling by Tup1 is strongly associated with Isw2 remodeling activity. (**A**) Pie graphs illustrating the association of 5′ Isw2-remodeling events with Tup1-remodeling events (remodeled defined as $r < 0.5$ for 1-kb window directly upstream from TSS). Graphs comparing Tup1-bound (Class SBU) promoters and unbound (Class NB) promoters. Association data was sorted by promoter class and Tup1-remodeling state. (Red box): Tup1-remodeled promoters. (Black box): Non Tup1-remodeled promoters. (Yellow): Percentage of promoters remodeled by Isw2. (Blue): Percentage of promoters not remodeled by Isw2. The 8% of unbound (NB) genes remodeled by Isw2 was expected and is consistent with the rate of genome wide 5′ Isw2 remodeling identified by Whitehouse and colleagues (60). (**B**) Average histone modification profiles from Pokholok *et al.* (68) for 1-kb window up and downstream of TSS. Promoters are sorted as unbound by Tup1 (Class NB) or Bound (combining Class SBB, SBU, WBB and WBU). All four Tup1-bound promoter classes were included in this analysis to increase the number of promoters with available TSS and modifications data. Additionally, Tup1-bound promoters are sorted according to downstream expression in *tup1*Δ strain (see 'Materials and Methods' section).

fragments (44). However, since MNase digestion does not release all nucleosomes at the same rate (68), the resulting mononucleosomal DNA population has a variable composition which depends largely on the extent of nuclease digestion (25). This variation presents a challenge of distinguishing genuine heterogeneity in nucleosome positions and occupancy/density between two chromatin populations from those created as an artifact of technical preparation, a dilemma increasingly encountered by chromatin biologists (69) and one made significantly more difficult when attempting comparisons between data sets from different laboratory groups, strains or organisms. Indeed, the brief comparison of genome-wide data sets in Supplementary Table S1 highlights the influence that subtle technical variations alone can exert between individual biological replicates from the same strain. While comparison of our *tup1*Δ data to samples from the Weiner *et al.* digestion series made in Supplementary Figure S7 represent intentional exaggerations of the influence that technical variation can yield on signal specificity, the low Tup1 enrichment (i.e. poor signal specificity) seen for all Weiner samples indicates that genome-wide data set correlations up to, and possibly exceeding, $r = 0.77$ are insufficient to achieve specific comparisons of chromatin structures.

Ultimately, the future of chromatin mapping studies requires an ability to make sensitive and specific comparisons between different chromatin states, be that strains, cell-types or environmental conditions, etc. to enhance our understanding of genome biology. Our matched MNase digestion approach was designed to accomplish this goal by reducing the technical variation introduced by the MNase digestion extent and gel extraction steps common in genome-wide chromatin mapping protocols. The procedure was successful in generating nucleosome maps that were essentially identical for the wild-type and *tup1Δ* strains sequenced, except for Tup1-specific differences in chromatin structure (Figure 2). More importantly, the specific differences in MNase protection our analysis identified were highly reproducible and related to changes in underlying nucleosome occupancy (Supplementary Figures S10–S12). Together, this data underscores the utility of matching the extent of MNase digestion as an approach to reduce technical variance in chromatin preparations and to enable accurate and reproducible downstream comparisons of chromatin structures.

Tup1 regulates chromatin at stress response genes

Comparison of TSS-aligned promoter MNase protection data indicates that Tup1's influence on chromatin

structure is primarily localized at upstream regulatory regions, specifically those associated with the Minus 1 and Minus 2 promoter nucleosomes (Figure 3C and D). Analysis of gene expression data also suggests that Tup1 promotes increased MNase protection at upstream locations to facilitate the repression of gene expression (Figure 6B). Additionally, analysis of clustering data indicates that decreases in MNase protection in a *tup1*Δ are associated with stress response pathways whereas increases in MNase protection are instead associated with translation and ribosome biogenesis pathways (Figure 6D–F and Supplementary Figure S13). Consistent with this, regulatory factors associated with both stress response and protein biosynthesis pathways show distinct Tup1-dependent chromatin structures overlying their binding sites *in vivo* (Figure 7). The effects of Tup1 regulation on chromatin structure at protein biosynthesis genes appears to be indirect (Supplementary Figure S14), however, multiple lines of evidence are presented which indicate that Tup1 regulates a distinct subset of these genes, as the characteristic Tup1 promoter structure is present for only the Tup1-bound fraction of protein biosynthesis genes (Supplementary Figures S13 and S14).

Tup1 has also been shown to regulate TF-binding specificity previously, whereby a nucleosomal hair-trigger blocks the conditional binding of a TF until the appropriate environmental signal is presented (41). Therefore, we attempted to identify the most likely TFs that could respond to Tup1-regulation through chromatin by examining the change in MNase protection centered on TFBSs (Figure 7). While our approach appears promising and identified the stress induced factor Xbp1 and the general stress response factors Msn2 and Msn4, this analysis is limited because the majority of the data for the bound TFBS were obtained in experiments preformed during growth in rich media (50). Further experiments with the appropriate environment for conditional activity of suspected TFs will be required to identify conditional TFBSs whose binding may be regulated by Tup1-dependent nucleosome occupancy. Additionally, Tup1 regulation of binding through chromatin will need to be confirmed by alternate approaches. However, from this analysis, it is clear that Tup1-dependent nucleosome occupancy specifically overlies the binding sites of many stress response factors and its own recruiters, presenting another link between chromatin structure regulation by Tup1 and stress–response pathways.

Chromatin remodeling by Tup1 represses transcription in conjunction with Isw2

Tup1–Ssn6-mediated repression is believed to operate through a multistep mechanism involving HDAC recruitment, interactions with hypoacetylated histones and transcription machinery, and cooperation with other chromatin remodeling complexes such as Isw2 (26). Combined mutations for genes encoding each of these factors have demonstrated larger effects on repression at individual loci *in vivo*, compared to single mutations, suggesting that cooperation between repressive factors enables separate, synergistic contributions to the regulation of genes (31). Moreover, unequal sensitivities of Tup1-regulated genes to the inactivation of different repression pathways *in vivo* also indicates that responses to Tup1 repression may vary in a gene-specific fashion, whereby different groups of genes have evolved different strategies for utilizing Tup1–Ssn6 repression mechanisms (28). Here, we show that a majority (52%) of Tup1-remodeled promoters are also Isw2-remodeled (Figure 8A), indicating that the majority of Tup1-remodeling may be caused by its interaction with Isw2. Results extend individual loci studies defining a Tup1 gene repression mechanism through Isw2-dependent nucleosome positioning (33,60) and demonstrate that this mechanism is functioning at many Tup1-regulated sites across the genome. Interestingly, an analysis of the association of site-specific Tup1 recruiting cofactors binding with Tup1-remodeling events demonstrated that nearly all Tup1 recruiting cofactors are associated with Tup1's activity on chromatin and that no single factor is solely responsible for directing Tup1's chromatin remodeling efforts. Additionally, the binding of Tup1, which follows the aforementioned recruiting efforts, is also not significantly predictive of which regions of chromatin Tup1 selects to remodel. Therefore, it is clear from our analysis that the specificity of Tup1 chromatin remodeling is not defined by Tup1 recruitment or binding alone and requires additional cellular inputs. Further examination, focusing on post-translational modifications of Tup1-associated cofactors and their corresponding signaling pathways should shed light on how certain sites in the genome can have their chromatin remodeled by Tup1 while other sites remain unaffected.

Tup1 targets open promoters to enhance downstream gene expression plasticity

Despite the variable roles Tup1 can play in regulating gene expression, Tup1-bound genes assume a distinct promoter packaging, consisting of low nucleosome occupancy/poorly positioned nucleosomes and a significantly wider NDR region (Figure 3C). Both the low nucleosome occupancy and wide NDR seen at Tup1-bound promoters in our study may reflect an abundance of easily digested nucleosomes at these loci that were digested away by our chromatin preparation or could reflect a more open chromatin structure overall. Regardless of the possibilities, it is clear from our analysis that Tup1-bound genes are structured significantly differently than the rest of the yeast genome. This distinct promoter packaging also includes a wider distribution of conserved TF-binding sites and these loci are targeted by a larger number of *trans*-activating factors *in vivo*. Together, this data demonstrates that Tup1 regulation requires inputs from more regulatory factors at distinct promoter locations compared to other transcriptional regulatory mechanisms active in *S. cerevisiae*.

Overall, the characteristic chromatin signature of Tup1-regulated genes is consistent with previous studies of chromatin structure identifying distinct nucleosome occupancy signatures in relation to transcriptional processes

(49), but what does this mean? Why does Tup1 selectively target open regulatory regions? From analysis in Figure 3C, we can see that Tup1 is not responsible for creating the distinct architecture at the genes it targets because deletion of Tup1 did not revert the Tup1-bound promoters to a narrower NDR promoter with increased nucleosome occupancy and improved positioning. Deletion of Tup1 instead caused the opposite effect, producing a significant decrease in MNase protection at the −1 and −2 promoter nucleosomes. Therefore, knowing that this distinctive chromatin structure is not reliant on Tup1 activity, we instead propose that Tup1 is targeted based on its unique ability to enhance downstream expression plasticity of these distinctly structured genes (Figure 5). We propose that the ability of Tup1 to bind to both active and repressed genes (26), the diverse DNA-binding partners solicited by Tup1 (42), the different regions of the Tup1–Ssn6 complex capable of interacting with DNA and protein partners (70), as well as the multiple mechanisms of transcriptional repression that Tup1 can elicit, all enable Tup1 to take advantage of these open promoters to promote downstream transcriptional plasticity. From our analysis, it seems likely that Tup1-dependent nucleosome occupancy is a key part of these transcriptional responses, as distinct changes in chromatin structure are seen at Tup1-regulated promoters depending on the associated gene expression program (Figure 6A–C), biological process (Figure 6D–F), or underlying regulatory factor-binding sites (Figure 7) involved.

SUPPLEMENTARY DATA

Supplementary Data are available at NAR Online.

FUNDING

National Science Foundation (grant IIS1016929 to M.J.B.); PhRMA predoctoral fellowship in Informatics (to J.M.R.) Funding for open access charge: SUNY at Buffalo Department of Biochemistry.

Conflict of interest statement. None declared.

REFERENCES

1. Radman-Livaja,M. and Rando,O.J. (2010) Nucleosome positioning: how is it established, and why does it matter? *Dev. Biol.*, **339**, 258–266.
2. Venters,B.J. and Pugh,B.F. (2009) How eukaryotic genes are transcribed. *Crit. Rev. Biochem. Mol. Biol.*, **44**, 117–141.
3. Li,B., Carey,M. and Workman,J.L. (2007) The role of chromatin during transcription. *Cell*, **128**, 707–719.
4. Kornberg,R.D. and Lorch,Y. (1999) Twenty-five years of the nucleosome, fundamental particle of the eukaryote chromosome. *Cell*, **98**, 285–294.
5. Luger,K., Mader,A.W., Richmond,R.K., Sargent,D.F. and Richmond,T.J. (1997) Crystal structure of the nucleosome core particle at 2.8 A resolution. *Nature*, **389**, 251–260.
6. Kamakaka,R.T. and Biggins,S. (2005) Histone variants: deviants? *Genes Dev.*, **19**, 295–310.
7. Kusch,T. and Workman,J.L. (2007) Histone variants and complexes involved in their exchange. *Subcell. Biochem.*, **41**, 91–109.
8. Sarma,K. and Reinberg,D. (2005) Histone variants meet their match. *Nat. Rev. Mol. Cell. Biol.*, **6**, 139–149.
9. Rando,O.J. (2007) Global patterns of histone modifications. *Curr. Opin. Genet. Dev.*, **17**, 94–99.
10. Albert,I., Mavrich,T.N., Tomsho,L.P., Qi,J., Zanton,S.J., Schuster,S.C. and Pugh,B.F. (2007) Translational and rotational settings of H2A.Z nucleosomes across the Saccharomyces cerevisiae genome. *Nature*, **446**, 572–576.
11. Stunkel,W., Kober,I. and Seifart,K.H. (1997) A nucleosome positioned in the distal promoter region activates transcription of the human U6 gene. *Mol. Cell. Biol.*, **17**, 4397–4405.
12. Lomvardas,S. and Thanos,D. (2002) Modifying gene expression programs by altering core promoter chromatin architecture. *Cell*, **110**, 261–271.
13. Lam,F.H., Steger,D.J. and O'Shea,E.K. (2008) Chromatin decouples promoter threshold from dynamic range. *Nature*, **453**, 246–250.
14. Wyrick,J.J., Holstege,F.C., Jennings,E.G., Causton,H.C., Shore,D., Grunstein,M., Lander,E.S. and Young,R.A. (1999) Chromosomal landscape of nucleosome-dependent gene expression and silencing in yeast. *Nature*, **402**, 418–421.
15. Sekinger,E.A., Moqtaderi,Z. and Struhl,K. (2005) Intrinsic histone-DNA interactions and low nucleosome density are important for preferential accessibility of promoter regions in yeast. *Mol. Cell.*, **18**, 735–748.
16. Kaplan,N., Moore,I.K., Fondufe-Mittendorf,Y., Gossett,A.J., Tillo,D., Field,Y., LeProust,E.M., Hughes,T.R., Lieb,J.D., Widom,J. *et al.* (2009) The DNA-encoded nucleosome organization of a eukaryotic genome. *Nature*, **458**, 362–366.
17. Yuan,G.C. and Liu,J.S. (2008) Genomic sequence is highly predictive of local nucleosome depletion. *PLoS Comput. Biol.*, **4**, e13.
18. Segal,E. and Widom,J. (2009) Poly(dA:dT) tracts: major determinants of nucleosome organization. *Curr Opin. Struct. Biol.*, **19**, 65–71.
19. Iyer,V. and Struhl,K. (1995) Poly(dA:dT), a ubiquitous promoter element that stimulates transcription via its intrinsic DNA structure. *EMBO J.*, **14**, 2570–2579.
20. Kornberg,R.D. and Stryer,L. (1988) Statistical distributions of nucleosomes: nonrandom locations by a stochastic mechanism. *Nucleic Acids Res.*, **16**, 6677–6690.
21. Mavrich,T.N., Ioshikhes,I.P., Venters,B.J., Jiang,C., Tomsho,L.P., Qi,J., Schuster,S.C., Albert,I. and Pugh,B.F. (2008) A barrier nucleosome model for statistical positioning of nucleosomes throughout the yeast genome. *Genome Res.*, **18**, 1073–1083.
22. Field,Y., Kaplan,N., Fondufe-Mittendorf,Y., Moore,I.K., Sharon,E., Lubling,Y., Widom,J. and Segal,E. (2008) Distinct modes of regulation by chromatin encoded through nucleosome positioning signals. *PLoS Comput. Biol.*, **4**, e1000216.
23. Workman,J.L. and Kingston,R.E. (1998) Alteration of nucleosome structure as a mechanism of transcriptional regulation. *Annu. Rev. Biochem.*, **67**, 545–579.
24. Clapier,C.R. and Cairns,B.R. (2009) The biology of chromatin remodeling complexes. *Annu. Rev. Biochem.*, **78**, 273–304.
25. Weiner,A., Hughes,A., Yassour,M., Rando,O.J. and Friedman,N. (2010) High-resolution nucleosome mapping reveals transcription-dependent promoter packaging. *Genome Res.*, **20**, 90–100.
26. Malave,T.M. and Dent,S.Y. (2006) Transcriptional repression by Tup1-Ssn6. *Biochem. Cell. Biol.*, **84**, 437–443.
27. Smith,R.L. and Johnson,A.D. (2000) Turning genes off by Ssn6-Tup1: a conserved system of transcriptional repression in eukaryotes. *Trends Biochem. Sci.*, **25**, 325–330.
28. Green,S.R. and Johnson,A.D. (2004) Promoter-dependent roles for the Srb10 cyclin-dependent kinase and the Hda1 deacetylase in Tup1-mediated repression in Saccharomyces cerevisiae. *Mol. Biol. Cell.*, **15**, 4191–4202.
29. Keleher,C.A., Redd,M.J., Schultz,J., Carlson,M. and Johnson,A.D. (1992) Ssn6-Tup1 is a general repressor of transcription in yeast. *Cell*, **68**, 709–719.

30. Courey,A.J. and Jia,S. (2001) Transcriptional repression: the long and the short of it. *Genes Dev.*, **15**, 2786–2796.
31. Zhang,Z. and Reese,J.C. (2004) Redundant mechanisms are used by Ssn6-Tup1 in repressing chromosomal gene transcription in Saccharomyces cerevisiae. *J. Biol. Chem.*, **279**, 39240–39250.
32. Li,B. and Reese,J.C. (2001) Ssn6-Tup1 regulates RNR3 by positioning nucleosomes and affecting the chromatin structure at the upstream repression sequence. *J. Biol. Chem.*, **276**, 33788–33797.
33. Zhang,Z. and Reese,J.C. (2004) Ssn6-Tup1 requires the ISW2 complex to position nucleosomes in Saccharomyces cerevisiae. *EMBO J.*, **23**, 2246–2257.
34. Fleming,A.B. and Pennings,S. (2001) Antagonistic remodelling by Swi-Snf and Tup1-Ssn6 of an extensive chromatin region forms the background for FLO1 gene regulation. *EMBO J.*, **20**, 5219–5231.
35. Kastaniotis,A.J., Mennella,T.A., Konrad,C., Torres,A.M. and Zitomer,R.S. (2000) Roles of transcription factor Mot3 and chromatin in repression of the hypoxic gene ANB1 in yeast. *Mol. Cell. Biol.*, **20**, 7088–7098.
36. Fleming,A.B. and Pennings,S. (2007) Tup1-Ssn6 and Swi-Snf remodelling activities influence long-range chromatin organization upstream of the yeast SUC2 gene. *Nucleic Acids Res.*, **35**, 5520–5531.
37. Gavin,I.M. and Simpson,R.T. (1997) Interplay of yeast global transcriptional regulators Ssn6p-Tup1p and Swi-Snf and their effect on chromatin structure. *EMBO J.*, **16**, 6263–6271.
38. Saito,S., Miura,S., Yamamoto,Y., Shindo,H. and Shimizu,M. (2002) The role of nucleosome positioning in repression by the yeast alpha 2/Mcm1p repressor. *Nucleic Acids Res.*, **2(Suppl.)**, 93–94.
39. Shimizu,M., Roth,S.Y., Szent-Gyorgyi,C. and Simpson,R.T. (1991) Nucleosomes are positioned with base pair precision adjacent to the alpha 2 operator in Saccharomyces cerevisiae. *EMBO J.*, **10**, 3033–3041.
40. Gavin,I.M., Kladde,M.P. and Simpson,R.T. (2000) Tup1p represses Mcm1p transcriptional activation and chromatin remodeling of an a-cell-specific gene. *EMBO J.*, **19**, 5875–5883.
41. Buck,M.J. and Lieb,J.D. (2006) A chromatin-mediated mechanism for specification of conditional transcription factor targets. *Nat. Genet.*, **38**, 1446–1451.
42. Hanlon,S.E., Rizzo,J.M., Tatomer,D.C., Lieb,J.D. and Buck,M.J. (2011) The stress response factors Yap6, Cin5, Phd1, and Skn7 direct targeting of the conserved co-repressor Tup1-Ssn6 in S. cerevisiae. *PLoS One*, **6**, e19060.
43. Buck,M.J., Nobel,A.B. and Lieb,J.D. (2005) ChIPOTle: a user-friendly tool for the analysis of ChIP-chip data. *Genome Biol.*, **6**, R97.
44. Rando,O.J. (2010) Genome-wide mapping of nucleosomes in yeast. *Methods Enzymol.*, **470**, 105–118.
45. Shivaswamy,S., Bhinge,A., Zhao,Y., Jones,S., Hirst,M. and Iyer,V.R. (2008) Dynamic remodeling of individual nucleosomes across a eukaryotic genome in response to transcriptional perturbation. *PLoS Biol.*, **6**, e65.
46. David,L., Huber,W., Granovskaia,M., Toedling,J., Palm,C.J., Bofkin,L., Jones,T., Davis,R.W. and Steinmetz,L.M. (2006) A high-resolution map of transcription in the yeast genome. *Proc. Natl Acad. Sci. USA*, **103**, 5320–5325.
47. Jiang,C. and Pugh,B.F. (2009) A compiled and systematic reference map of nucleosome positions across the Saccharomyces cerevisiae genome. *Genome Biol.*, **10**, R109.
48. Pugh,B.F. (2010) A preoccupied position on nucleosomes. *Nat. Struct. Mol. Biol.*, **17**, 923.
49. Lee,W., Tillo,D., Bray,N., Morse,R.H., Davis,R.W., Hughes,T.R. and Nislow,C. (2007) A high-resolution atlas of nucleosome occupancy in yeast. *Nat. Genet.*, **39**, 1235–1244.
50. Harbison,C.T., Gordon,D.B., Lee,T.I., Rinaldi,N.J., Macisaac,K.D., Danford,T.W., Hannett,N.M., Tagne,J.B., Reynolds,D.B., Yoo,J. *et al.* (2004) Transcriptional regulatory code of a eukaryotic genome. *Nature*, **431**, 99–104.
51. MacIsaac,K.D., Wang,T., Gordon,D.B., Gifford,D.K., Stormo,G.D. and Fraenkel,E. (2006) An improved map of conserved regulatory sites for Saccharomyces cerevisiae. *BMC Bioinformatics*, **7**, 113.
52. Liu,X., Lee,C.K., Granek,J.A., Clarke,N.D. and Lieb,J.D. (2006) Whole-genome comparison of Leu3 binding in vitro and in vivo reveals the importance of nucleosome occupancy in target site selection. *Genome Res.*, **16**, 1517–1528.
53. Liu,C.L., Kaplan,T., Kim,M., Buratowski,S., Schreiber,S.L., Friedman,N. and Rando,O.J. (2005) Single-nucleosome mapping of histone modifications in S. cerevisiae. *PLoS Biol.*, **3**, e328.
54. Tirosh,I. and Barkai,N. (2008) Two strategies for gene regulation by promoter nucleosomes. *Genome Res.*, **18**, 1084–1091.
55. Gasch,A.P., Spellman,P.T., Kao,C.M., Carmel-Harel,O., Eisen,M.B., Storz,G., Botstein,D. and Brown,P.O. (2000) Genomic expression programs in the response of yeast cells to environmental changes. *Mol. Biol. Cell.*, **11**, 4241–4257.
56. Martinez-Pastor,M.T., Marchler,G., Schuller,C., Marchler-Bauer,A., Ruis,H. and Estruch,F. (1996) The Saccharomyces cerevisiae zinc finger proteins Msn2p and Msn4p are required for transcriptional induction through the stress response element (STRE). *EMBO J.*, **15**, 2227–2235.
57. Schmitt,A.P. and McEntee,K. (1996) Msn2p, a zinc finger DNA-binding protein, is the transcriptional activator of the multistress response in Saccharomyces cerevisiae. *Proc. Natl Acad. Sci. USA*, **93**, 5777–5782.
58. Gorner,W., Durchschlag,E., Martinez-Pastor,M.T., Estruch,F., Ammerer,G., Hamilton,B., Ruis,H. and Schuller,C. (1998) Nuclear localization of the C2H2 zinc finger protein Msn2p is regulated by stress and protein kinase A activity. *Genes Dev.*, **12**, 586–597.
59. Whitehouse,I., Rando,O.J., Delrow,J. and Tsukiyama,T. (2007) Chromatin remodelling at promoters suppresses antisense transcription. *Nature*, **450**, 1031–1035.
60. Tomar,R.S., Psathas,J.N., Zhang,H., Zhang,Z. and Reese,J.C. (2009) A novel mechanism of antagonism between ATP-dependent chromatin remodeling complexes regulates RNR3 expression. *Mol. Cell. Biol.*, **29**, 3255–3265.
61. Whitehouse,I. and Tsukiyama,T. (2006) Antagonistic forces that position nucleosomes in vivo. *Nat. Struct. Mol. Biol.*, **13**, 633–640.
62. Bone,J.R. and Roth,S.Y. (2001) Recruitment of the yeast Tup1p-Ssn6p repressor is associated with localized decreases in histone acetylation. *J. Biol. Chem.*, **276**, 1808–1813.
63. Davie,J.K., Trumbly,R.J. and Dent,S.Y. (2002) Histone-dependent association of Tup1-Ssn6 with repressed genes in vivo. *Mol. Cell. Biol.*, **22**, 693–703.
64. Davie,J.K., Edmondson,D.G., Coco,C.B. and Dent,S.Y. (2003) Tup1-Ssn6 interacts with multiple class I histone deacetylases in vivo. *J. Biol. Chem.*, **278**, 50158–50162.
65. Wu,J., Suka,N., Carlson,M. and Grunstein,M. (2001) TUP1 utilizes histone H3/H2B-specific HDA1 deacetylase to repress gene activity in yeast. *Mol. Cell.*, **7**, 117–126.
66. Watson,A.D., Edmondson,D.G., Bone,J.R., Mukai,Y., Yu,Y., Du,W., Stillman,D.J. and Roth,S.Y. (2000) Ssn6-Tup1 interacts with class I histone deacetylases required for repression. *Genes Dev.*, **14**, 2737–2744.
67. Pokholok,D.K., Harbison,C.T., Levine,S., Cole,M., Hannett,N.M., Lee,T.I., Bell,G.W., Walker,K., Rolfe,P.A., Herbolsheimer,E. *et al.* (2005) Genome-wide map of nucleosome acetylation and methylation in yeast. *Cell*, **122**, 517–527.
68. Bryant,G.O., Prabhu,V., Floer,M., Wang,X., Spagna,D., Schreiber,D. and Ptashne,M. (2008) Activator control of nucleosome occupancy in activation and repression of transcription. *PLoS Biol.*, **6**, 2928–2939.
69. Kaplan,N., Hughes,T.R., Lieb,J.D., Widom,J. and Segal,E. (2010) Contribution of histone sequence preferences to nucleosome organization: proposed definitions and methodology. *Genome Biol.*, **11**, 140.
70. Tzamarias,D. and Struhl,K. (1994) Functional dissection of the yeast Cyc8-Tup1 transcriptional co-repressor complex. *Nature*, **369**, 758–761.